sustainability

MDPI

Article

Seismic Resilience Assessment Strategy for Social and Sustainability Impact Evaluation on Transportation Road Network: A Seismic Liquefaction-Induced Damage Application

Mauro D'Apuzzo [1], Azzurra Evangelisti [1,*], Rose Line Spacagna [1], Giuseppe Cappelli [1,2], Vittorio Nicolosi [3], Giuseppe Modoni [1] and Luca Paolella [1]

1 Department of Civil and Mechanical Engineering, University of Cassino and Southern Lazio, Via G. Di Biasio 43, 03043 Cassino, Italy; dapuzzo@unicas.it (M.D.); rlspacagna@unicas.it (R.L.S.); giuseppe.cappelli1@unicas.it (G.C.); modoni@unicas.it (G.M.); paolella@unicas.it (L.P.)
2 University School for Advanced Studies, IUSS, Piazza della Vittoria 15, 27100 Pavia, Italy
3 Department of Enterprise Engineering "Mario Lucertini", University of Rome "Tor Vergata", Via del Politecnico 1, 00133 Rome, Italy; nicolosi@uniroma2.it
* Correspondence: aevangelisti.ing@gmail.com

Abstract: Transport networks play a critical role for living communities, as they facilitate the exchange of people and goods and foster economic growth. Improving their resilience against seismic hazards, among which liquefaction is by far one of the most significant and complex, is consistent with most of the Sustainable Development Goals pinpointed by the United Nations' Agenda. In this paper, an original methodological framework, combining innovative Geo-statistical approaches to analyze soil properties, prediction models for soil liquefaction, and calibrated transport demand models providing the social and economic cost associated with seismic-induced road damages and closures within a renewed Geographical Information Systems (GIS) workspace, is proposed. In particular, based on traditional risk assessment evaluation, an innovative approach to evaluate the exposure in terms of economic loss due to lack of accessibility is presented. The methodology is applied to a district area in northern Italy that underwent a recent seismic event that caused several soil liquefaction phenomena. Results provided by a sensitivity analysis on a stochastic (return period) basis are derived: as the seismic intensity increases, the total social costs increase, but the trend of the rates due to traffic delays and the loss of accessibility are irregular. Although further simulation scenarios need to be undertaken, the proposed methodology seems to provide an effective planning tool to evaluate preventive strategies aimed at improving the resilience of transport networks against liquefaction risk.

Keywords: seismic resilience; transportation network; social cost; embankments; serviceability; liquefaction

check for updates

Citation: D'Apuzzo, M.; Evangelisti, A.; Spacagna, R.L.; Cappelli, G.; Nicolosi, V.; Modoni, G.; Paolella, L. Seismic Resilience Assessment Strategy for Social and Sustainability Impact Evaluation on Transportation Road Network: A Seismic Liquefaction-Induced Damage Application. *Sustainability* **2022**, *14*, 8411. https://doi.org/10.3390/su14148411

Academic Editors: Dashnor Hoxha, Wu Wei and Ancuţa Rotaru

Received: 16 June 2022
Accepted: 4 July 2022
Published: 8 July 2022

1. Introduction

Transport infrastructure networks represent one of most significant systems affecting the quality of life and economic development of human communities. However, because of their extensive layout, they undergo several natural and/or anthropogenic threats and/or hazards that may impact their functionality and, in turn, the involved communities nearby.

For these reasons, in the last two decades, several national and international projects and research studies have been promoted with the aim of evaluating transportation network risk assessment and to estimate the potential losses induced by natural and man-made catastrophic events [1–10], and other more recent studies implementing GIS environment have been presented for vulnerability assessment [11,12].

According to a traditional engineered approach that is mainly based on risk evaluation, thus far the main interest has focused on the Expected Annual Damage (EAD) and Expected Annual Exposure (EAE) [13], where the former parameter refers to repair/replacements losses due to disruption events.

However, nowadays, a leap forward is required to cope with adverse events that cannot be tackled within the traditional risk-based approach. The focus of transport managers is to shift from prevention against threats or events that may occur and that may degrade the performance of the asset itself to a new comprehensive "Resilience-based" approach, able to speed up recovery and restore initial (ex ante) asset conditions, once the disruptive events have occurred [14].

Following the derivative of a concept initially grown within structural mechanics, resilience, intended as the "ability to recovery from adversities or disturbances", has been extended to a wider range of fields, such as psychology, ecology, sociology, urban planning, and so on [15,16]. Within the civil engineering context, since early 2000, resilience has been recalled in transportation networks, mainly with reference to response to natural hazards; however, it should be acknowledged that a resilience-based approach should embrace all type of risks (natural and man-derived risks) [13].

Although resilience in transport networks has been the subject of a several reviews [17,18], a common background can be identified encompassing two main aspects: the ability to maintain functionality under disruptions or degrading scenarios, and the time and resources required to restore the level of performance after disruptions. Basing on these premises, Resilience may be defined as the ability of a transport system to prepare for and adapt to major disruption, provide and maintain an acceptable level of service or functionality, and respond to and recover rapidly from disruption. Currently, there is no measurement standard for resilience within the transportation network and the resilience metrics for transportation infrastructure used thus far can be divided into two categories: topological (TOP) metrics and performance-based (PB) metrics, where the latter metrics are considered more appropriate than topological metrics as the TOP approach does not consider flows in the networks [14].

On the other hand, it must be acknowledged that the United Nations recently proposed a strategic plan to foster the 2030 agenda for sustainable development goals (SDGs) [19]. In this connection, increasing resilience of transport networks against natural hazards seems consistent with SDG9 (Industry Innovation and Infrastructures) and SDG11 (Sustainable Cities and Communities), but it may also impact other SDGs. For instance, road closures following disruption events may affect accessibility to small communities and this, in turn, will impact SDG8 (Decent Work and Economic Growth) and/or will increase inequalities among communities themselves (SDG9), whereas corresponding traffic delays will be responsible for an increase in exhaust emissions by motor vehicles, worsening air quality, which will affect SDG3 (Good Health and Well-being), SDG15 (Life on Land), and climate change and corresponding Climate Action (SDG13).

Among the natural hazards stressing the transport networks, seismic-related hazards are by far most significant. In this connection, transport infrastructure damage induced by soil liquefaction phenomena appears to deserve a higher focus due to their extensive character, especially in liquefaction prone soil formations.

In this paper, an original complex methodological framework, combining innovative Geo-statistical approaches to analyze soil properties, soil liquefaction prediction models, and calibrated transport demand models providing the social and economic cost associated with seismic-induced road closures within a renewed Geographical Information Systems workspace, is proposed. The methodology that is described in the following section is applied to a district area in northern Italy that underwent a recent seismic event that caused several soil liquefaction phenomena.

2. Methodology

Seismic risk assessment quantifies the probability of occurrence and associated uncertainty on seismic intensity, ground motion, subsoil condition, infrastructure response, physical damage, and socio-economic losses. A flow chart of the proposed methodology is reported in the following figure (Figure 1).

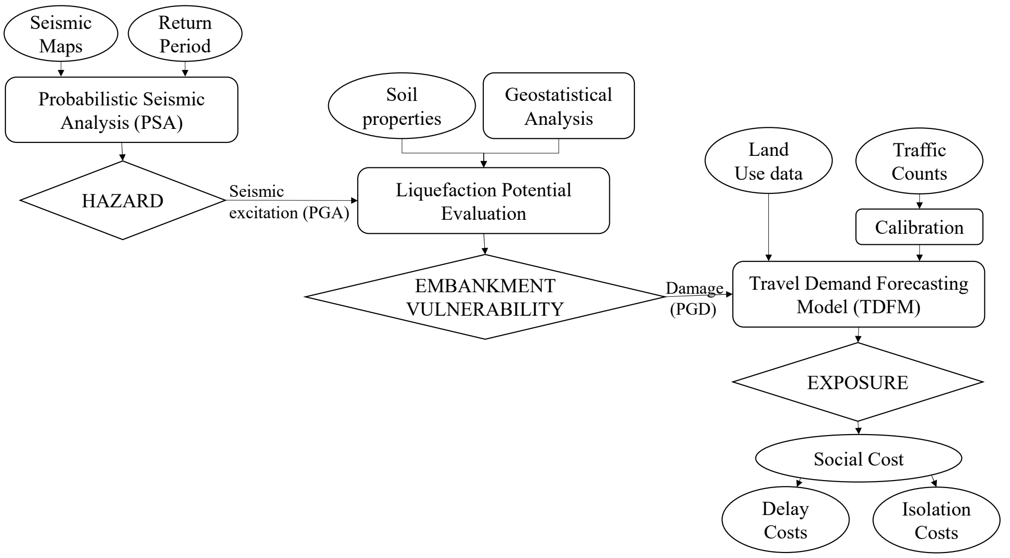

Figure 1. Conceptual Flow Chart of the proposed methodology.

In detail, the methodology can be summarized into the synthetic formal Equation (1):

$$R = f\{H,\ V,\ E\} \quad (1)$$

where:

R = Risk;
H = Hazard;
V = Vulnerability;
E = Exposure.

The proposed methodology is applied to local site effects induced by seismic liquefaction of the foundation soil and focuses on the transportation network's response in terms of socio-economic losses.

Regarding the liquefaction *Hazard*, the predisposing factors of the seismic liquefaction are the intensity of the earthquake and the subsoil conditions. In particular, liquefaction occurs in saturated sandy soils with limited fine content and low density. The main effect of soil liquefaction is the reduction in the bearing capacity of the soil. On transportation road networks, this phenomenon can produce irregular settlements, causing local damage able to impact network functionality and socio-economic activities. Therefore, according to the proposed methodology, the coupled analysis, characterized by subsoil–infrastructural interaction responses, proposed by Karamitros et al. [20], is applied to compute the liquefaction-induced settlements on road embankments.

In fact, the analytical formula of Karamitros et al. [20] enables computation of the seismic settlements of strip and rectangle footings (and embankments may be assimilated to a such element) resting on liquefiable soil with a clay crust. This settlement is associated with a "sliding-block" type of punching failure through the clay crust and within the liquefied sand layer. The basic idea is that liquefaction-induced settlements are dynamically correlated with seismic excitation characteristics and the post-shaking degraded static factor of safety. Additionally, the effect of shear-induced dilation of the liquefied subsoil is considered. The adopted model combines the bounding surface plasticity theory with a vanished elastic region to predict all fundamental aspects of the monotonic and the cyclic response and liquefaction of sands.

The proposed expression for the dynamic settlement ρ_{dyn} (i.e., the settlement during shaking) is shown in Equation (2), with ca being a foundation aspect ratio correction (where $c' = 0.003$), a_{max} the peak bedrock acceleration, T the representative period of the motion, N

the number of cycles of the excitation, Z_{liq} the thick liquefiable sand layer, B the embankment width at the base, and FS_{deg} the degraded static factor of safety of the foundation.

$$\rho_{dyn} = ca_{max}T^2N\left(\frac{Z_{liq}}{B}\right)^{1.5}\cdot\left(\frac{1}{FS_{deg}}\right)^3 \quad (2)$$

$$c = c'\left(1 + 1.65\cdot\frac{L}{B}\right) \leq 11.65c' \quad (3)$$

$$a_{max}T^2N = \int_{t=0}^{t}|v(t)|dt \quad (4)$$

FS_{deg} in Equation (2) can be calculated as the degraded bearing capacity ($q_{ult,deg}$) divided by the bearing pressure (q) (see Equation (6)), which is evaluated in each section by multiplying the soil unit weight g for the transversal area of the embankment. The foundation bearing capacity failure mechanism is simulated by the Meyerhof and Hanna model [21] for a crust on a weak layer using the degraded friction angle in Equation (5) where r_u is the average excess pore pressure ratio of the liquefied sand and φ_0 is the initial friction angle. The superficial crust is beneficial, and there is an upper bound beyond where failure occurs entirely within the crust and is not affected by the liquefiable layer.

$$\varphi_{deg} = tan^{-1}(1 - r_u)tan(\varphi_0) \quad (5)$$

$$FS_{deg} = \frac{q_{ult,deg}}{q} \quad (6)$$

As far as the road embankment *Vulnerability* assessment is concerned, the SYNER-G classification for the definition of the damage state limits [22] is adopted. In particular, it considers three different levels of damage state:

1. *Minor*, characterized by an average Permanent Ground Deformation (PGD) of 0.05 m [min 0.02 m ÷ max 0.08 m]. Generally, the observed damages on the road are surface slide of the embankment at the top of the slope, minor cracks on the road surface, and/or minor track displacement. The related road network serviceability includes a useful road, open to vehicle traffic, with a speed reduction.
2. *Moderate*, characterized by an average PGD of 0.15 m [min 0.08 m ÷ max 0.22 m]. Generally, the observed damages on the road are deep slide or slump of the embankment, medium cracks on the road surface and/or settlement, and/or medium track displacement. The related road network serviceability includes a partially open road during repair works with an alternating direction of vehicle traffic.
3. *Extensive,* characterized by an average PGD of 0.4 m [min 0.22 m ÷ max 0.58 m]. Generally, the observed damages on the road are extensive slump and slide of the embankment, extensive cracks on the road surface and/or settlement, and/or extensive tracks displacement. The related road network serviceability includes a complete unusable road, closed to vehicle traffic.

Finally, the concept of transport network *Exposure* is expressed as the quantification of the socio-economic damages that a catastrophic event, such as liquefaction, can produce to the collectivity. It is intimately linked to the Social Costs concept, which can be usually evaluated as a sum of direct (i.e., repair or replacement cost of the damaged elements) and indirect (reduction in or interruption of the transportation network service and its consequences on society and economy) losses.

As far as the characterization of the analysis of transportation networks is concerned, according to the level of assessment of their functionality, a transportation network analysis classification has been proposed [4] and is summarized in Table 1.

Table 1. Summary of the transportation network analysis classification [4].

Transportation Network Analysis Type	Description
Vulnerability	related to the damage level of each single element of the transportation network (such as bridge, tunnel, embankment, etc.), according to a specific post-seismic scenario.
Connectivity	according to a specific post-earthquake scenario, evaluates the accessibility to specific or strategic areas when the loss of service of some connections occurs.
Capacity	related to the network capacity to accommodate traffic flows, and provides direct and indirect losses due to damage levels occurring in the whole network.
Serviceability	provides a more realistic estimate of total loss in the long-term, taking into account both direct and indirect impacts on economic sectors.

In the methodology here presented, a preliminary approach for a simplified Serviceability Analysis is proposed. It has been conceived with the aim to evaluate indirect losses due to reduced/ceased activity in economic sectors (industry, services, life activities) and losses due to increased travel time, both caused by the loss of accessibility to the inhabited center.

In fact, in the scenarios of complete isolation of the inhabited center, socio-economic impacts are accounted for in the reduction in or interruption of all socio-economic activities such as the closure of schools, commercial activities, offices, and industries in the isolated inhabited center.

The simplified approach proposed for the assessment of socio-economic losses is presented below.

2.1. Assessment of Socio-Economic Losses: A Simplified Approach

As previously mentioned, the complete Serviceability Analysis applied to a generic catastrophic scenario can provide a more realistic estimate of total loss, including both direct losses related to physical damage suffered by the built environment (network components, residential, business, and industrial buildings) and indirect losses caused by the increased travel time of the traffic network and the reduction in or closure of economic activities [4].

It is worth noting that, as far as the complete Serviceability Analysis application is concerned, the complexity of the economic models becomes relevant (and their analysis is not the aim of this paper), and the quantity and quality of the input data become onerous. Its fully systemic analysis involves the knowledge of information relating to the variation in the demand in terms of both travel (the increasing travel times make trips less attractive) and goods, commodities, services, etc. (due to damaged factories and industries, isolation of inhabited centers, etc.). Finally, all these considerations must be modeled depending on the speed of the reconstruction and/or recovery process [23].

Due to the complexity of collecting input data and evaluating economic models, the simplified methodology for the assessment of indirect losses here proposed has the purpose of providing a satisfactory evaluation of indirect socio-economic losses.

It is based on the estimation of two fundamental categories of socio-economic losses, which can be directly related to the economic and social sectors of an inhabited or an industrial/business area:

- indirect losses due to the impact on traffic mobility due to the temporary reduced functionality of the transportation network;
- indirect losses due to the temporary isolation of the inhabited and/or industrial/business center.

Below, a more detailed description is provided.

2.1.1. Evaluation of Indirect Losses Due to the Increasing Travel Costs

The temporary reduction in and/or loss of serviceability of the transportation networks, which can mainly depend on the level of damage, the features of the transportation system, and the traffic demand, has as a principal consequence an impact on the traffic flows and the trips of the study area.

In order to evaluate socio-economic impacts related to mobility in the post-catastrophic scenario, the indirect losses in terms of the Total Delay Cost, *TDC*, are estimated. Assuming that the Generalized Transport Cost, *GTC*, is a measure of the overall cost (including travel time cost) that is "paid" by each transport user in a specific study area, the *TDC* can be evaluated using the following expression (7):

$$TDC = GTC_{post} - GTC_{pre} \tag{7}$$

where:

TDC = Total Delay Cost computed on a daily basis;

GTC_{post} = Generalized Transport Cost in the post-seismic scenario;

GTC_{pre} = Generalized Transport Cost in the pre-seismic scenario.

In order to evaluate the aliquot of social cost suffered by a community in the study area, due to the impact of traffic delays, *TDC* must be multiplied by the overall number of days needed to restore the pre-seismic event conditions of the transportation network.

The evaluation of the delay related to the damage impact on the transportation system requires the development and implementation of the Travel Demand Forecasting Model, TDFM, which, according to Cascetta [24], is a mathematical four-stage model which reproduces, on an hourly basis, all the trips occurring in a specific analysis area, according to its purpose (*s*), user class (*cu*), time period (*h*), origin (*o*), destination (*d*), transport mode (*m*), and path (*k*).

In particular, the TDFM can be evaluated by means of the following equation [24]:

$$d^i_{od}(s,h,m,k) = d^i_o(sh) \cdot p^i(d/osh) \cdot p^i(m/oshd) \cdot p^i(k/oshdm) \tag{8}$$

where:

$d^i{}_{od}(s, h, m, k)$ is the average number of trips performed by cu_i, starting from origin traffic zone *o*, finishing in the destination traffic zone *d*, for a specific purpose *s*, within the time period *h*, using the transport mode *m*, and choosing the trip path *k*;

$d^i{}_o(sh)$ is the average number of cu_i that perform a trip from *o*, for purpose *s*, within the time period *h*;

$p^i(d/osh)$ is the fraction of the cu_i that travels to *d* performing a trip from *o*, for purpose *s*, within the time period *h*;

$p^i(m/oshd)$ is the fraction of the cu_i that uses the transport mode *m*, performing a trip from *o* to *d*, for purpose *s*, within the time period *h*;

$p^i(k/oshdm)$ is the fraction of the cu_i that chooses the trip path *k*, performing a trip from *o* to *d*, for purpose *s*, within the time period *h*, with the transport mode *m*.

2.1.2. Evaluation of Indirect Losses Due to the Isolation of the Inhabited and/or Industrial/Business Center

In the case of very disruptive catastrophic events, an entire inhabited center and/or industrial and economic center has a high probability of remaining isolated from the rest of the road network. The causes can be both of a direct nature, when there is direct damage to the road infrastructure, and when the damage to the built environment occludes the roads with rubble. In both cases, the accessibility is compromised for a time that depends on the nature and extension of the damage, and it is necessary to estimate the economic losses suffered by the community.

The simplified approach here proposed is based on the evaluation of two main economic features of the society:

1. Lost income due to lost days of work;
2. Lost income due to lost days of school.

In the first case, the lost income can be easily evaluated as the number of lost days of work for each worker included in the isolated area (considering both workers in the area who live outside and who live in the study area but have a job outside), multiplying for the relative daily wage. It is possible to perform different levels of accuracy of the analysis: considering various annual income brackets with the relative number of workers, or considering an average annual income value of the area, applied for all the present workers. This annual income so estimated can be used to evaluate daily income of the area, which, multiplied for the isolation days of the inhabited center and/or industrial and economic center, provides the lost income due to lost days of work. Equation (9) estimates lost income due to lost days of work:

$$LI_{LDW} = \frac{AAI}{an_{wd}} \cdot nd_i \cdot nw_{ia} \tag{9}$$

where:

LI_{LDW} = Lost income due to the lost days of work [EUR];
AAI = Average annual labor income of the area [EUR];
an_{wd} = Average number of working days in a year [dimensionless];
nd_i = Number of days of isolation of the area [dimensionless];
nw_{ia} = Number of workers in the isolated area [dimensionless].

In the second case, the lost income can be evaluated as the number of lost days of school for each student included in the isolated area, multiplying for the relative future daily expected wage. This economic characteristic is based on the concept of human capital, which can be defined as "*the stock of knowledge, skills and other personal characteristics embodied in people that helps them to be productive*" [25]. For this reason, to invest in human capital, formal education, from early childhood to formal school systems and adult training programs, must be encouraged. At the same time, missing long periods of education would negatively affect the human capital of each student, affecting their future wage.

The relationship between wages and years of education is defined by the wage–education curve, which indicates the levels of future expected wages for each level/year of education achieved. Different curves can be developed for each country, year, and type of schooling.

Equation (10) estimates the lost income due to lost days of school:

$$LI_{LDS} = \frac{AEFI}{an_{sd}} \cdot nd_i \cdot ns_{ia} \tag{10}$$

where:

LI_{LDS} = Lost income due to the lost days of school [EUR];
$AEFI$ = Average expected future income level of the area [EUR];
An_{sd} = Average number of school days in a year [dimensionless];
nd_i = Number of days of isolation of the area [dimensionless];
ns_{ia} = Number of students in the isolated area [dimensionless].

The methodology described thus far is applied in a case study presented below.

3. Case Study

The Emilian Po Valley (Italy) was, in 2012, subjected to a series of severe seismic events, which, after the two major events occurred on May 20th (Mw = 6.1-hypocentral depth of 6.3 km) and on May 29th (Mw = 5.8-hypocentral depth of 10.2 km), caused a total of 27 victims, around 400 injured, more than 15,000 displaced persons, and extensive damage to the cultural and economic heritage of the area. Furthermore, due to the particular conditions of the subsoil, widespread liquefaction phenomena were observed.

In the area of the municipalities of San Carlo, Sant'Agostino, and Mirabello, called Terre del Reno, along the old riverbed of the Reno River, the greatest concentration of liquefaction evidence has been detected [26].

In Figure 2, the area of Terre del Reno, its municipalities, and the position of the two major seismic events that occurred in 2012, are reported.

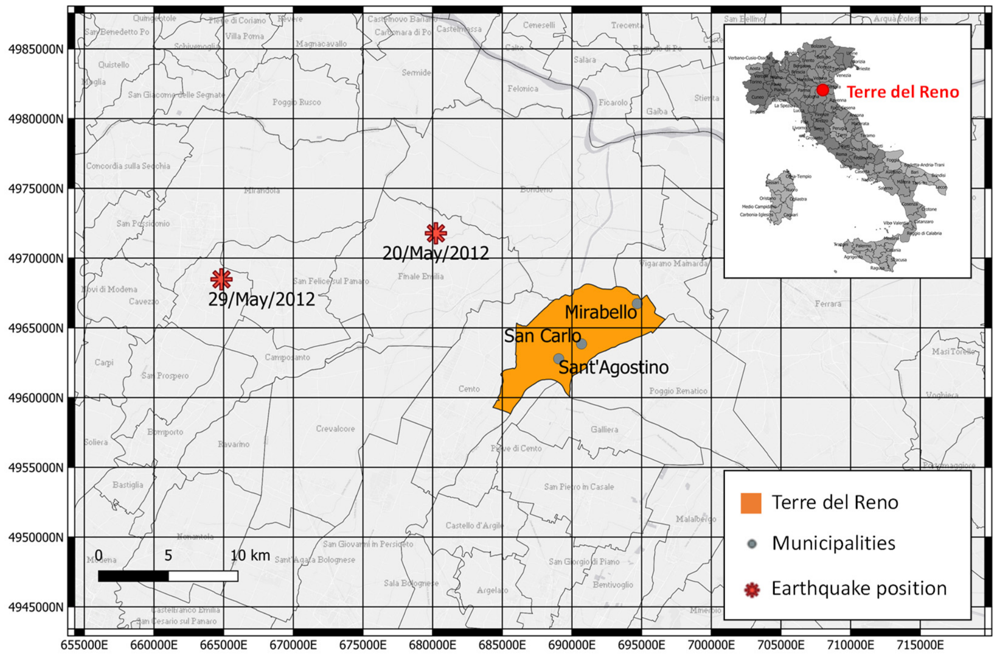

Figure 2. The Terre del Reno area, the municipalities of Sant'Agostino, San Carlo, and Mirabello, and the position of the two major seismic events occurred in 2012.

These urban areas and their relative road networks were built near the paleo-channel and paleo-levees of the Reno River, where the subsoil can be categorized into (from the top down): fluvial channel deposits, a stratum of fine-grained materials (swamps), and Pleistocene alluvial plain. Finally, in order to protect the territories against flooding, artificial silty sand layers have been built along the old riverbed.

Due to the importance of the series of seismic events and the numerous and relevant observations of liquefaction phenomena, the area of Terre del Reno was therefore selected as the case study for the application of the methodology previously introduced.

3.1. Liquefaction Phenomenon and Damage Evaluation

Sand with limited fine content, and sufficiently low density and saturation, coupled with a relatively high regional seismicity, are paramount factors for the occurrence of liquefaction. Additionally, according to the liquefaction hazard assessment proposed in [27], a coupled approach for subsoil and infrastructural responses has been adopted. In fact, by comparison with an effective stress calculation performed with an advanced numerical model [28], the formula of Karamitros et al., 2013 [20] has been adapted to compute the liquefaction-induced settlements of embankments of Terre del Reno.

For a probabilistic approach, four increasing seismic events have been simulated for the road network damage evaluation, in addition to the real event of 20 May 2012. In particular, Return Periods (RPs) of 30, 50, 475, and 975 years have been selected, and in Figure 3 are reported the five road network damage levels for each RP.

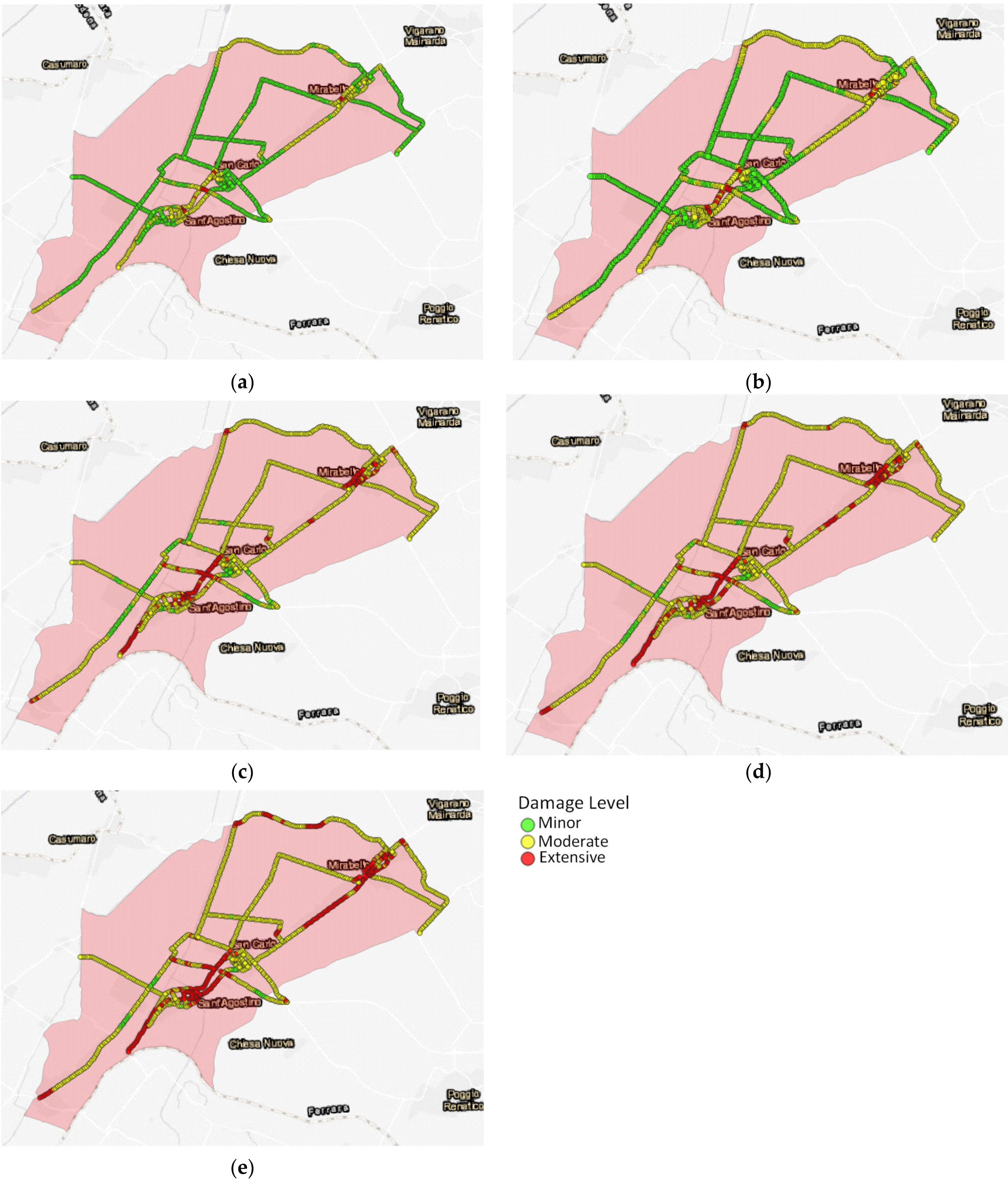

Figure 3. Maps of the embankment damage levels for (**a**) RP 30Y, (**b**) RP 50Y, (**c**) Back-Analysis, (**d**) RP 475Y, and (**e**) RP 975Y.

3.2. Travel Demand Forecasting Model of Terre del Reno

In order to evaluate the social cost suffered by the Terre del Reno territory, the TDFM of Terre del Reno was developed. The prominent presence of trough traffic, which characterizes Terre del Reno, means that, after a sensitivity analysis (see [29]), the study area is of at least 60 km of radius. Therefore, the TDFM was developed, calibrated, and experimentally validated in a buffer area of 60 km of radius around a rural area located in the district of Terre del Reno [29]. In Figure 4, the graph of the study area is reported.

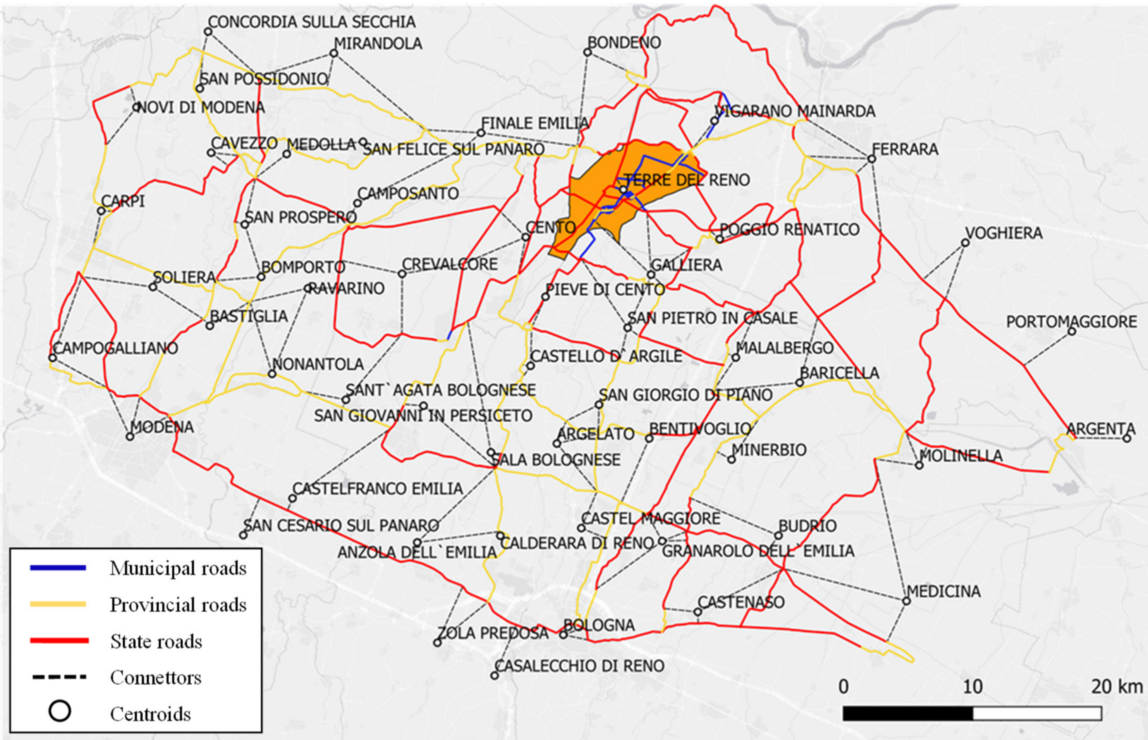

Figure 4. Graph of the study area.

In particular, the daily fluctuation of the mobility is partitioned considering three "hourly" scenarios: a "peak" scenario that occurs mainly in two time slots (from 7:00 to 9:00 and from 17:00 to 19:00), a "median peak" (from 12:00 to 14:00), and an "off-peak" for the rest of the day.

The Origin/Destination (O/D) matrix was preliminarily developed based on commuter mobility data derived from the 2011 Census promoted by Italian National Institute of Statistics (ISTAT) [30] which contain only systematic commuting trip data and corresponding modal split. Finally, the O/D matrixes (different for each hourly scenarios) was calibrated with traffic counts provided by the Emilia-Romagna Region [31].

By way of example, in Figure 5 the results of the TDFM calibration, in terms of traffic flows for the morning peak hour, are reported.

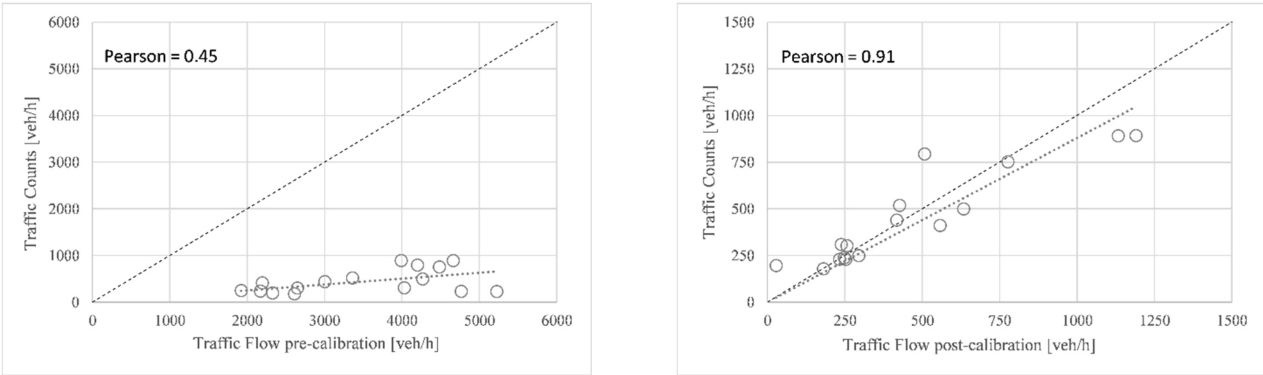

(**a**) (**b**)

Figure 5. Comparison of Traffic Counts vs. Predicted Traffic Flow (**a**) pre-calibration and (**b**) post-calibration.

Observing Figure 5, it is possible to see that the traffic flow estimates of the pre-calibration phase (derived from the commuter mobility data [30]) overestimate the real traffic flow. This could be due to having neglected, in the traffic model, the presence of the A 13 motorway. This difference is conveniently corrected by the traffic model calibration (see Figure 5b).

In order to convert the traffic delay into Overall Social Cost, a cost o45EUR 45 for heavy vehicles and EUR 12 for the others, is applied.

3.3. Socio-Economic Aspects of Terre del Reno District for Indirect Losses Evaluation

As previously mentioned, Terre del Reno is a district composed by three different municipalities: Sant'Agostino, San Carlo, and Mirabello (see Figure 2). In order to apply the simplified approach for the evaluation of indirect losses due to the isolation of the inhabited and/or industrial/business center, few and simple socio-economic data were collected from the ISTAT open-source databases and are summarized in Table 2.

Table 2. Summary of the socio-economic features of Terre del Reno district [32,33].

Population	N° Workers	Average Annual Wage of the Area [EUR]	N° Students
10.571	7.778	19.592	5.180

It should be noted that both workers who move to and from Terre del Reno district to carry out their work have been considered.

Finally, in order to evaluate the average expected annual salary for Terre del Reno district, the wage–education curve was estimated. According to data analyzed by the Bank of Italy [34] for the Italian population, the wage–education curve for the year 2012, corresponding to the seismic event year, is represented in Figure 6.

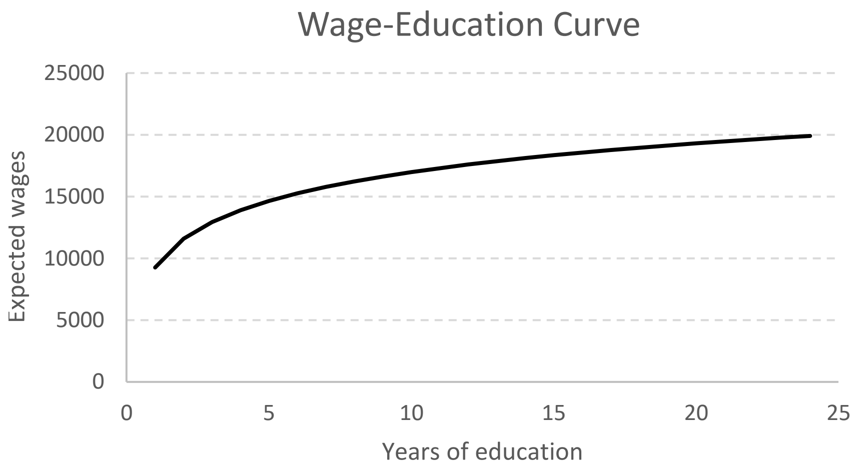

Figure 6. Italian wage–education curve for the year 2012.

Therefore, assuming an average schooling course of 12 years for the Terre del Reno district, an average expected annual salary of approximately EUR 17,600 is obtained.

4. Results

For each return period scenario, including the real event of 20 May 2012, a traffic analysis on the road network, according to the relative suffered damage level, has been performed. By way of example, the results for the morning peak hour, in terms of distribution of traffic flows, are summarized in Figure 7.

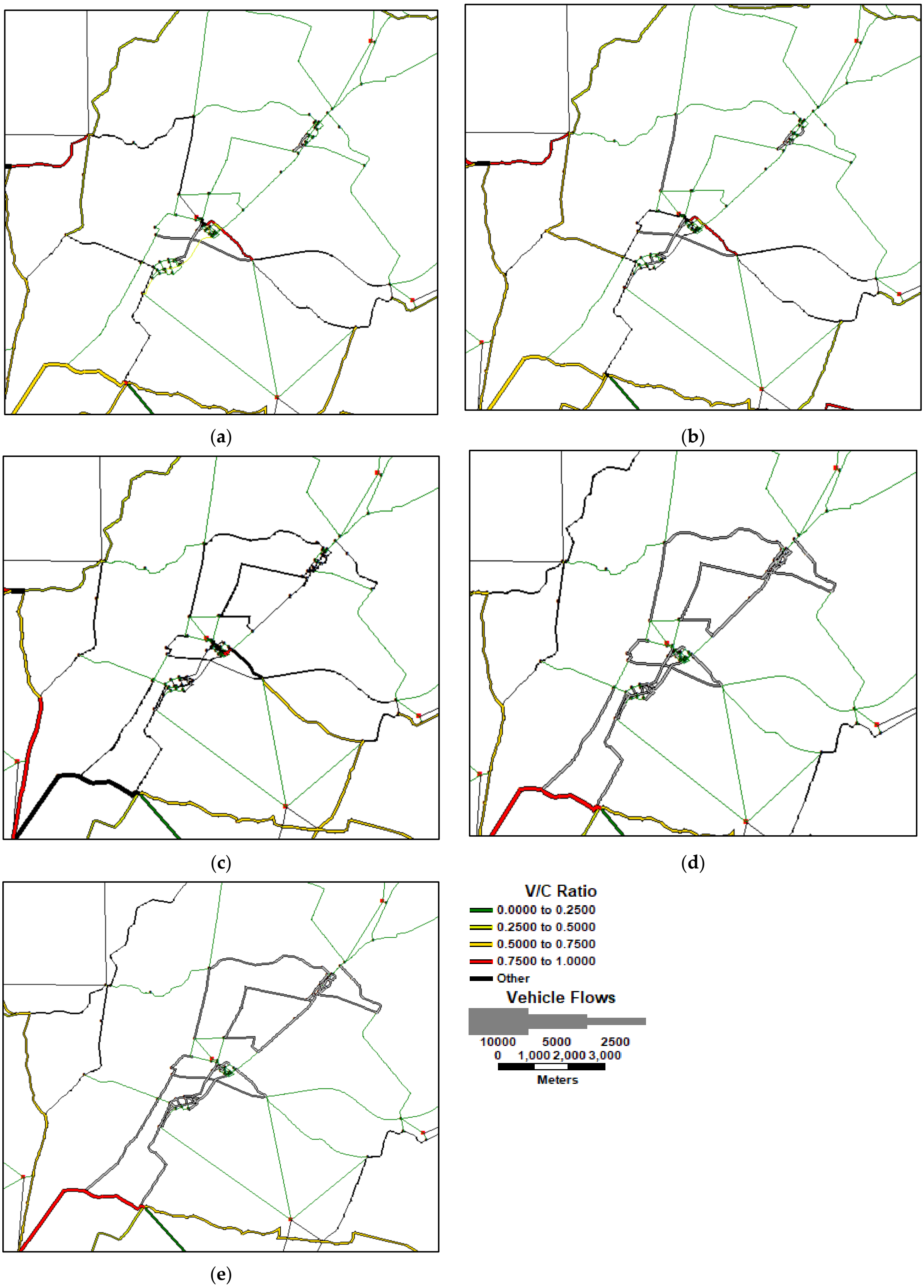

Figure 7. Distribution of traffic flows on Terre del Reno district for (**a**) RP 30Y, (**b**) RP 50Y, (**c**) Back-Analysis, (**d**) RP 475Y, and (**e**) RP 975Y.

As it is possible to observe from Figure 7, the seismic events characterized by the last two RPs cause the complete isolation of the Terre del Reno district; in fact, accessibility to the three distinct municipalities is lost. For only these seismic scenarios, evaluation of indirect losses due to the isolation of Terre del Reno district is performed.

By means of Equation (7), the TDC, and in turn, the aliquot of social cost due to the impact of traffic delays are evaluated. Then, applying Equations (9) and (10), the aliquot of social costs due to the lost income for lost days of work and school are calculated. The results are summarized in the Table 3.

Table 3. Summary of the results in terms of traffic delays and social costs suffered by Terre del Reno district for the return periods.

Return Period	Traffic Delays (TDs) [h]	Social Cost Due to TDs [EUR]	Social Cost Due to Isolation [EUR]	Total Social Cost [EUR]
30 Years	1014	34,354,989	-	34,354,989
50 Years	1118	38,003,367	-	38,003,367
20 May 2012 Event	1636	62,481,661	-	62,481,661
475 Years	1063	46,689,300	17,398,797	64,088,097
975 Years	1019	48,569,595	22,966,412	71,536,007

It is important to highlight that the isolation period, which coincides with the time needed to restore accessibility to Terre del Reno district, is assessed by assuming focused and partial restoration activities, with the sole aim of re-establishing accessibility to the three main municipalities as soon as possible.

5. Discussions

As it is possible to see in the summary of Table 3, in the last two analyzed return periods, a reduction, in terms of both traffic delay and the relative aliquot of social cost, is highlighted. While it may seem counterintuitive, the reduction is correctly related to the damage level suffered by the road network. In fact, in the last two return period scenarios, complete isolation of the Municipality of Terre del Reno occurred. In these particular cases, a considerable number of trips, which generally take place in the territory of Terre del Reno, are suppressed. These lost trips are also a cost suffered by the community, which must renounce the movements of its normal everyday life.

In order to assess the aliquot of social cost which reflects the overall number of lost trips, in the seismic scenarios of RP 475 years and 975 years, indirect losses due to the isolation of Terre del Reno district are evaluated.

According to the simplified approach here proposed, for the evaluation of indirect losses due to the isolation of Terre del Reno, only lost income due to lost days of work and school are considered.

It is worth highlighting that the results presented in this work are focused on evaluation of indirect losses in terms of social costs and do not include the evaluation of direct costs due to the reconstruction.

It is believed that this kind of cost may represent a better candidate for a resilience-based seismic retrofitting budget allocation methodology within a transportation asset management system.

6. Conclusions

In this paper, a new approach for the evaluation of indirect economic losses due to the isolation of the inhabited and/or industrial/business center, and due to traffic delays suffered by a community after a catastrophic event, was proposed.

The strategy is part of the liquefaction risk assessment methodology, which, also by means of geoinformatics [35], involves the evaluation and combination of the territorial distribution of hazard, vulnerability, and exposure [27].

Then, a probabilistic approach was performed on Terre del Reno district, by simulating five different seismic events with increasing return periods (from 30 years to 975 years, including the real event of 20 May 2012). The liquefaction damage levels suffered by the road network and the relative road network serviceability, according to the SYNER-G classification [22], were evaluated and, for each scenario, a traffic analysis, to evaluate the travel time, was performed. Finally, according to the simplified approach here presented, the social costs, in terms of both traffic delay impact and indirect losses due to the isolation of Terre del Reno, were evaluated.

Results obtained thus far, according to what is expected, confirm that as the seismic intensity of the event increases, the traffic delays suffered by the community increase, until the isolation of the Municipality occurred. In this case, the number of suppressed trips "lightens" the pressure of road traffic on the network but, at the same time, it causes increasing social costs paid by the community, which were evaluated as indirect economic costs due to the isolation of the inhabited and/or industrial/business center.

It should be noted that, although the methodology here presented was applied to liquefaction risk evaluation, the proposed approach for the evaluation of indirect economic losses due to the isolation of the inhabited and/or industrial/business center, and due to traffic delays, can be applied to the evaluation of other natural and/or man-made disrupting events.

Although further simulation scenarios need to be undertaken, the proposed methodological framework seems to provide an effective planning tool to evaluate preventive strategies and budget allocation prioritization criteria for seismic retrofitting aimed at improving the resilience of transport networks against catastrophic risk. Future research can be oriented to the application of the proposed methodology to develop road asset management tools that can drive highway managers in planning seismic retrofitting road interventions in a more "resilient" way.

Author Contributions: Conceptualization, M.D., A.E., R.L.S. and G.M.; methodology, M.D., A.E., R.L.S. and G.M.; software, A.E., R.L.S. and L.P.; validation, A.E., R.L.S. and L.P.; formal analysis, A.E., R.L.S. and L.P.; investigation, A.E., R.L.S. and L.P.; resources, A.E., R.L.S. and L.P.; data curation, A.E., R.L.S., G.C. and L.P.; writing—original draft preparation, A.E., R.L.S.; writing—review and editing, M.D.; G.M. and V.N.; visualization, A.E., R.L.S., G.C. and L.P.; supervision, M.D.; G.M. and V.N.; project administration, G.M.; funding acquisition, G.M. All authors have read and agreed to the published version of the manuscript.

Funding: This research received no external funding. The APC was funded by the Erasmus+ project KA2—Higher education strategic partnerships No. 2018-1-RO01-KA203-049214, "Rehabilitation of the Built Environment in the Context of Smart City and Sustainable Development Concepts for Knowledge Transfer and Lifelong Learning"—RE-BUILT.

Conflicts of Interest: The authors declare no conflict of interest. The funders had no role in the design of the study; in the collection, analyses, or interpretation of data; in the writing of the manuscript, or in the decision to publish the results.

References

1. Kaundinya, I.; Nisancioglu, S.; Kammerer, H.; Oliva, R. All-hazard guide for transport infrastructure. *Transp. Res. Procedia* **2016**, *14*, 1325–1334. [CrossRef]
2. STRIT Project Homepage. Available online: http://www.stress-scarl.com/it/innovazione/i-progettinazionali/strit.html (accessed on 1 June 2022).
3. *Multi-Hazard Loss Estimation Methodology Earthquake Model HAZUS®MH MR4 Technical Manual*; National Institute of Building Sciences. (NIBS): Washington, DC, USA, 2003; Available online: http://www.civil.ist.utl.pt/~{}mlopes/conteudos/DamageStates/hazus_mr4_earthquake_tech_manual.pdf (accessed on 1 June 2022).
4. Pitilakis, K.; Argyroudis, S.; Kakderi, K.; Argyroudi, A. Systemic seismic vulnerability and risk analysis for buildings, lifeline networks and infrastructures safety gain. *SYNER-G Synth. Document JRC Sci. Policy Rep.* **2013**, *10*, 23242. [CrossRef]

5. Molarius, R.; Tuomaala, P.; Piira, K.; Räikkönen, M.; Aubrecht, C.; Polese, M.; Zuccaro, G.; Pilli-Sihvola, K.; Rannat, K. Systemic Vulnerability and Resilience Analysis of Electric and Transport Network Failure in Cases of Extreme Winter Storms. In *Vulnerability, Uncertainty, and Risk: Quantification, Mitigation, and Management*; American Society of Civil Engineers (ASCE): Reston, VA, USA, 2014; pp. 608–617.
6. Krieger, J.; Kohl, B.; Žibert, M.; Dolenc, D. Security Manual for European Road Infrastructure. Copyright: SecMan Consortium. 2013. Available online: https://www.bast.de/EN/Publications/Media/B-sicherheitshandbuch-eng-l.html (accessed on 1 June 2022).
7. Security of Road Transport Networks. Copyright: 2009–2012 SeRoN Consortium. 2012. Available online: https://cordis.europa.eu/project/id/225354/reporting/de (accessed on 1 June 2022).
8. Seville, E.; Nicholson, A. Risk and Impact of Natural Hazards on a Road Network. *J. Transp. Eng.* **2001**, *127*, 159–166. [CrossRef]
9. Werner, S.D.; Taylor, C.E.; Cho, S.; Lavoie, J.-P.; Huyck, C.; Eitzel, C.; Chung, H.; Eguchi, R.T. *Redars 2 Methodology and Software for Seismic Risk Analysis of Highway Systems*; Special Report MCEER-06-SP08; Federal Highway Administration: Washington, DC, USA, 2006.
10. Chang, L. Transportation System Modeling and Applications in Earthquake Engineering. Doctoral Thesis, The Graduate College of the University of Illinois at Urbana-Champaign, Champaign, IL, USA, 2010.
11. Leggieri, V.; Mastrodonato, G.; Uva, G. GIS Multisource Data for the Seismic Vulnerability Assessment of Buildings at the Urban Scale. *Buildings* **2022**, *12*, 523. [CrossRef]
12. Ji, J.; Cui, H.; Zhang, T.; Song, J.; Gao, Y. A GIS-based tool for probabilistic physical modelling and prediction of landslides: GIS-FORM landslide susceptibility analysis in seismic areas. *Landslides* **2022**, *2022*, 1–19. [CrossRef]
13. Koks, E.E.; Rozenberg, J.; Zorn, C.; Tariverdi, M.; Vousdoukas, M.; Fraser, S.A.; Hall, J.W.; Hallegatte, S. A global multi-hazard risk analysis of road and railway infrastructure assets. *Nat. Commun.* **2019**, *10*, 2677. [CrossRef] [PubMed]
14. Nicolosi, V.; Augeri, M.; D'Apuzzo, M.; Evangelisti, A.; Santilli, D. A Probabilistic Approach to the Evaluation of Seismic Resilience in Road Asset Management. *Int. J. Disaster Risk Sci.* **2022**, *13*, 114–124. [CrossRef]
15. Werner, E.E. *Vulnerable but Invincible: A Longitudinal Study of Resilient Children and Youth*; McGraw-Hill: New York, NY, USA, 1989; ISBN 0937431036.
16. Pickett, S.T.A.; Cadenasso, M.L.; Grove, J.M. Resilient cities: Meaning, models, and metaphor for integrating the ecological, socio-economic, and planning realms. *Landsc. Urban Plan.* **2004**, *69*, 373. [CrossRef]
17. Flannery, A.; Pena, M.A.; Manns, J. *Resilience in Transportation Planning, Engineering, Management, Policy, and Administration*; No. Project 20-05; Topic 48-13; National Academies of Sciences, Engineering, and Medicine: Washington, DC, USA, 2018.
18. Zhou, Y.; Wang, J.; Yang, H. Resilience of Transportation Systems: Concepts and Comprehensive Review. *IEEE Trans. Intell. Transp. Syst.* **2019**, *20*, 4262–4276. [CrossRef]
19. Sachs, J.; Schmidt-Traub, G.; Kroll, C.; Lafortune, G.; Fuller, G.; Woelm, F. *Sustainable Development Report 2020*; Cambridge Books: Cambridge, UK, 2021.
20. Karamitros, D.K.; Bouckovalas, G.D.; Chaloulos, Y.K. Seismic settlements of shallow foundations on liquefiable soil with a clay crust. *Soil Dyn. Earthq. Eng.* **2013**, *46*, 64–76. [CrossRef]
21. Meyerhof, G.G.; Hanna, A.M. Ultimate bearing capacity of foundations on layered soils under inclined load. *Can. Geotech. J.* **1978**, *15*, 565–572. [CrossRef]
22. Pitilakis, K.; Crowley, H.; Kaynia, A.M. SYNER-G: Typology definition and fragility functions for physical elements at seismic risk. *Geotech. Geol. Earthq. Eng.* **2014**, *27*, 1–28. [CrossRef]
23. Karaca, E. Regional Earthquake Loss Estimation: Role of Transportation Network, Sensitivity and Uncertainty, and Risk Mitigation. Ph.D. Thesis, Massachusetts Institute of Technology (MIT), Cambridge, MA, USA, 2005.
24. Cascetta, E. *Transportation Systems Analysis: Models and Applications*, 2nd ed.; Springer Science & Business Media: Berlin/Heidelberg, Germany, 2009; Volume 29, pp. 1–752. [CrossRef]
25. OECD, Organisation for Economic Cooperation and Development. Available online: https://www.oecd.org/economy/human-capital/ (accessed on 1 April 2022).
26. Fioravante, V.; Giretti, D.; Abate, G.; Aversa, S.; Boldini, D.; Capilleri, P.P.; Vannucchi, G. Earthquake geotechnical engineering aspects: The 2012 Emilia-Romagna earthquake (Italy). In Proceedings of the 7th International Conference on Case Histories in Geotechnical Engineering, Invited Lecture No. EQ-5, Wheeling, IL, USA, 29 April–4 May 2013; pp. 1–34.
27. D'Apuzzo, M.; Esposito, A.; Evangelisti, A.; Spacagna, R.L.; Paolella, L.; Modoni, G. Strategies for the assessment of risk induced by seismic liquefaction on road networks. In Proceedings of the 29th European Safety and Reliability Conference, Hannover, Germany, 22–26 September 2019; pp. 3277–3285. [CrossRef]
28. Modoni, G.; Spacagna, R.L.; Paolella, L.; Salvatore, E.; Rasulo, A.; Martelli, L. Liquefaction risk assessment: Lesson learned from a case study. In *Earthquake Geotechnical Engineering for Protection and Development of Environment and Constructions*; CRC Press: Boca Raton, FL, USA, 2019; pp. 761–774.
29. D'Apuzzo, M.; Evangelisti, A.; Modoni, G.; Spacagna, R.L.; Paolella, L.; Santilli, D.; Nicolosi, V. Simplified approach for liquefaction risk assessment of transportation systems: Preliminary outcomes. In *International Conference on Computational Science and Its Applications*; Springer: Cham, Switzerland, 2020; pp. 130–145. [CrossRef]
30. Italian Institute of Statistic (ISTAT). Origin/Destination Commuting Matrix, Year 2011. Available online: https://www.istat.it/it/archivio/139381 (accessed on 1 April 2022).
31. Emilia Romagna Region. Available online: https://servizissiir.regione.emilia-romagna.it/FlussiMTS/ (accessed on 1 April 2022).

32. Italian Institute of Statistic (ISTAT). Population and Households Census 2011. Available online: https://www.istat.it/it/archivio/104317 (accessed on 1 April 2022).
33. Italian Institute of Statistic (ISTAT). Irpef Taxable Incomes (Ipef)–Municipalities (Tax Year 2012). Available online: http://dati.istat.it/Index.aspx?DataSetCode=MEF_REDDITIIRPEF_COM (accessed on 1 April 2022).
34. Bank OF Italy. Survey on Household Income and Wealth—2012 Supplements to the Statistical Bulletin-Sample Surveys. Available online: https://www.bancaditalia.it/pubblicazioni/indagine-famiglie/bil-fam2012/index.html (accessed on 1 April 2022).
35. Spacagna, R.L.; Rasulo, A.; Modoni, G. Geostatistical analysis of settlements induced by groundwater extraction. In *International Conference on Computational Science and Its Applications*; Springer: Cham, Switzerland, 2017; pp. 350–364. [CrossRef]